

**Investigation of human exposure to triclocarban after showering, and
preliminary evaluation of its biological effects**

(Supporting Information)

Nils Helge Schebb, Bora Inceoglu, Ki Chang Ahn, Christophe Morisseau, Shirley Gee
and Bruce D. Hammock*

University of California, Davis, Department of Entomology and Cancer Center, One
Shields Avenue,
95616 Davis, California, USA,

* Corresponding author: Bruce D. Hammock
Department of Entomology
University of California at Davis
One Shields Avenue
Davis, CA 95616 USA
Tel: 530 752 7519
Fax: 530-751-1537
E-mail: bdhammock@ucdavis.edu

Summary: Details of methods and results pertaining to the LC-MS analyses of TCC its metabolites, oxylipins and the enzyme inhibition assays are provided in the SI. Moreover detailed results are presented in 6 tables and 13 figures.

Material and methods

Online-SPE-LC-MS

TCC and its metabolites (Fig. S1) were analysed by online SPE. Analysis (Fig. S2) was performed on a Agilent 1200 LC system comprised of two G1379B degasers, two G1312B gradient HPLC pumps and a high-pressure two-position six port valve attached in a G1316B column oven set to 40°C. Samples were kept at 4°C in a LEAP HTC-PAL auto sampler (Leap Technologies, Carrboro, NC) equipped with a 20 µL sample loop and 25 µL syringe. The samples (25 µL) were injected and 20 µL was introduced by full-loop injection into a flow of 1250 µL/min 0.1% acetic acid (AA) in water delivered by pump 1 (Fig. S2A). The analytes were extracted using a Cyclone RP-18 column (Thermo Fisher Scientific, Waltham, MA) with the dimensions 50 X 0.5 mm, a particle size of 50 µm and a pore size of 10 nm (Fig. S2A). After 1.0 min, the 6 port valve was switched, and the analytes were back flushed by the solvent stream of 300 µL/min delivered by pump 2 (Fig. S2II) into an Acquity C18 reversed phase (RP) column (Waters Milford, MA) with the dimensions 2.1 X 50 mm a particle size of 1.7 µm and a pore size of 13 nm. The analytes were separated by a binary gradient of 25 mM ammonium acetate containing 0.1 % acetic acid (HAc) as solvent A and pure acetonitrile (ACN) as solvent B. The gradient, the flow rates and the six port switching times are displayed in Fig. S2.

Mass spectrometric detection was carried out on an ABI 4000 TRAP tandem mass spectrometer equipped with a pneumatically assisted “turbo V” electrospray ionisation (ESI)-source (Applied Biosystems, Foster City, CA). The instrument was operated in negative ion mode with an ion-spray voltage of -2500V, using 25 psi curtain gas, 40 psi nebulizer gas and 70 psi drying gas at a temperature of 450°C. The ³⁵Cl isotopes of the analytes were detected in unit resolution in the selected reaction monitoring mode (SRM) with a dwell time of 50 ms, separated in two periods of 0-2.7 min and 2.7-7 min to increase the number of datum points of each peak. The transitions and the specific electronic parameters are shown in table S1. The collision-activated dissociation gas was set to “medium” and the entrance potential was 10 V for all analytes. All source parameters were optimized for TCC under LC conditions and the electronic parameters were optimized for each analyte by direct infusion. Fragment spectra of standards were recorded in direct infusion mode with ramped collision energy.

Analyst Software (version 1.4.4.2, Applied Biosystems) was used for controlling the online-SPE-LC-ESI-MS/MS system, data acquisition, integration and quantification. The analyte concentrations of the samples were calculated directly by comparison of the analyte peak area detected with that of the I.S. For calibration, the analyte to I.S. ratios were fitted in a linear way reciprocally weighted by concentration.

Ion suppression analysis was conducted by post-column mixing of the eluate with a flow of TCC solution (100 nM in 50/50; ACN/water) at 10 µL/min delivered by a syringe

pump. The TCC signal after injection of water and blank plasma and urine samples was monitored.

For qualitative analysis of *N*-glucuronides, urine was diluted with ACN 1:1 (v/v) and centrifuged. To increase the injected concentration of *N*-glucuronides acidified (addition of 0.1 vol. % acetic acid) urine was also extracted ethyl acetate. Three extractions with equal volume allowed an almost complete extraction from the urine. For qualitative urine analysis the LC was operated as standard gradient system, using the above mentioned stationary and mobile phases with the following gradient program: 0-0.5 min isocratic 10% B, 0.5-6.0 min linear from 10-100% B, 6.0-6.8 min isocratic 100%B and reconditioning for 2 minutes. ESI(-)-MS detection (declustering potential -70 V) was carried out either (i) in full scan mode (300-800 amu with a cycle time of 0.2 sec) or (ii) in enhanced product ion mode (EPI) on *m/z* of 489, 491 and 493 respectively generating high quality fragment spectra (spread collision energy (CE) -5– -35, scan range 100-500 amu) by operating the third quadruple as linear ion trap or (iii) in SRM mode with a optimized CE of -15 V and collision cell exit potential of -9 V using the transitions *m/z* 489→336 for the *N*-TCC-glucuronide and *m/z* 489→302 for the *N'*-TCC-glucuronide, respectively.

Optimization of conjugate hydrolysis

Since no reference standards for the TCC-N-Gs were available, the TCC amount bound in these conjugates had to be quantified after hydrolysis. To find and optimize the most appropriate hydrolysis conditions both acid hydrolysis as earlier described for TCC conjugates^{1, 2} as well as enzymatic hydrolysis with three different glucuronidases (GUS) have been carried out. Therefore urine samples containing a high concentration of TCC-NGs as well as standard solutions of the analytes were incubated with HCl (1 M) for various durations. In addition, glucuronidase (GUS) solutions containing 10,000 units of enzyme were prepared freshly in 1 M ammonium acetate buffer (pH 5.0) for the GUS type I and II from *Helix pomatia* and in 100 mM potassium phosphate buffer (pH 6.0) for GUS type VA from *E. coli* and mixed 1:9 with the samples. The hydrolysis rate during incubations at 37 °C was determined by LC-MS.

The incubation of a urine sample with a high concentration of TCC-N-Gs show, that the enzymes GUS-I and GUS-II from *Helix pomatia* completely cleaved TCC-*N*-Glucuronide within 14 h of incubation (1,000 U/mL enzyme, 37°C), whereas the TCC-*N'*-Glucuronide was largely resistant to hydrolysis with these enzymes (Fig. S3). Thus, incubations with these standard enzymes used in bio-monitoring of xenobiotics is not suitable for the complete detection of TCC released from TCC-N-Gs.

In contrast, GUS from *E. coli* Type VA completely cleaved both TCC-N-Gs after 6 h incubation (1,000 U/ml, 37°C). Acid hydrolysis by 10 minutes of incubation (1 M HCl, 100 °C) also fully cleaved both TCC-N-Gs. However, as already described by Gruenke et al. the carbanilides are not entirely stable towards acids¹. Following prolonged incubations at 100 °C with 1 M HCl a breakdown of TCC and its analogs was observed

(Fig. S3-4). The acid stability of the TCC congeners with the chlorine substitution were higher with a half life of 65 min for DCC, 85 min for TCC and 120 minutes for 3'-Cl-TCC. Consistent with previous findings, the half life of the hydroxylated 3'-OH-TCC and 2'-OH-TCC were 50 and 60 minutes, respectively, significantly shorter than the non-hydroxylated compounds (Fig. S3)¹. Nonetheless, the analytes are sufficiently stable to render the acid hydrolysis as the favourable hydrolysis technique, because of its speed and cost effectiveness compared to enzymatic hydrolysis. A 20 min incubation was chosen for the urine analysis, to ensure on the one hand a full cleavage of both TCC-N-Gs and on the other hand a low loss of analytes by acid degradation (<10% for TCC, and <20% for 2'-OH-TCC). For plasma analysis, where only small sample amounts were available, overnight incubation with GUS Type VA from *E. coli* was chosen as the hydrolysis technique and rat plasma (18 µL) was mixed with 2 µL GUS from *E. coli* and incubated overnight at 37 °C in 0.5 mL plastic tubes.

Human subjects

TCC exposure was investigated in a group of six healthy volunteers. Prior to the study, all subjects stated that there were healthy to the best of their knowledge and were well educated (at least a masters degree in a science related field). Information about sex, weight, height and age of the volunteers are provided in table S3. The body surface area of the volunteers was calculated according to the Mosteller formula³

LC-MS oxylipin analysis

An internal standard solution containing deuterated standards was added into 200 μ L plasma aliquots of the plasma samples. This was followed by extraction of the analytes on a preconditioned solid phase extraction column (60 mg waters Oasis-HLB, Waters, Milford, MA). The eluted samples were evaporated to dryness and reconstituted in 50 μ L of methanol. A 10 μ L aliquot of the reconstructed sample solution was directly analyzed by LC-ESI-MS/MS. Separation was carried out in 21 minutes on a Agilent 1200 SL LC system (Palo Alto, CA), utilizing a Agilent Zorbax Eclipse Plus C-18 reversed phase column (dimensions 2.1 x 150 mm, particle size 1.8 μ M) using the following gradient of 0.1% acetic acid as solvent A and 80/15/0.1 acetonitrile/methanol/acetic acid as solvent B at a flow rate of 0.25 mL/min: 0-0.25 min isocratic 35% B, 0.25-1.00 min linear from 35% B to 45% B, 1.00-3.00 min linear from 45% B to 55% B, 3.00-8.50 min linear from 55% B to 66% B, 8.50-12.50 min linear from 66% B to 72% B, 12.50-15.00 min linear from 72% B to 82% B, 15.00-16.50 min linear from 82% B to 95% B, 16.50-18.00 min isocratic 95% B, 18.00-18.10 min linear from 95% B to 35% followed by reconditioning for 3.40 min.

The detection was carried out using a 4000 QTRAP instrument (Applied Biosystems, Foster City, CA) operating in negative ion mode as previously described by monitoring the following SRM transitions: 9(10)-EpOME (m/z 295/171), 9,10-DiHOME (m/z 313/201), 12(13)-EpOME (m/z 295/195), 12,13-DiHOME (m/z 313/183), 8(9)-EpETrE (m/z 319/167), 8,9-DiHETrE (m/z 337/127), 11(12)-EpETrE (m/z 319/167), 11,12-DiHETrE (m/z 337/167), 14(15)-EpETrE (m/z 319/219), 14,15-DiHETrE (m/z 337/207), 8(9)-EpETE (m/z 317/127), 8,9-DiHETE (m/z 335/127), 11(12)-EpETE (m/z 317/167), 11,12-DiHETE (m/z 335/167), 14(15)-EpETE (m/z 317/207), 14,15-DiHETE (m/z 335/207), 17(18)-EpETE (m/z 317/215), 17,18-DiHETE (m/z 335/247), 10(11)-EpDPE (m/z 343/153), 10,11-DiHDPE (m/z 361/153), 13(14)-EpDPE (m/z 343/193), 13,14-DiHDPE (m/z 361/193), 16(17)-EpDPE (m/z 343/233), 16,17-DiHDPE (m/z 361/233), 19(20)-EpDPE (m/z 343/241) and 19,20-DiHDPE (m/z 361/273).

Calculation of the extreme values of urinary excretion of TCC

The total amount of TCC (m_{TCC}) and creatine (m_{crea}) urinary excreted results from the sum of the concentration (c_i) and the volume (V_i) of the samples (equations 1-2). With n number of the samples.

$$\text{eq. 1} \quad m_{TCC} = \sum_{i=1}^n c_{i_{TCC}} \cdot V_i$$

$$\text{eq. 2} \quad m_{Crea} = \sum_{i=1}^n c_{i_{crea}} \cdot V_i$$

The volume of the samples ($1 - n$) is unknown, thus the total amount of excreted TCC can not be calculated. However, based on assumed constant creatinine excretion ($m_{crea} = 1.5 \text{ g/24 h}$) and a realistic total volume for each sample, the highest and lowest total TCC excretion can be estimated:

For a sample k the volume can be expressed by combination of eq.1 and 2 and subsequent rearrangement as:

$$\text{eq. 3} \quad V_k = \frac{1}{c_{k_{crea}}} \cdot \left(m_{crea} - \sum_{\substack{i=1 \\ i \neq k}}^n c_{i_{crea}} \cdot V_i \right)$$

Substitution V_i in eq. 1 by V_k :

$$\text{eq. 4} \quad m_{TCC} = \sum_{\substack{i=1 \\ i \neq k}}^n c_{i_{TCC}} \cdot V_i + c_k \cdot V_k$$

and expression of v_k by eq. 3 leads to:

$$\text{eq. 5} \quad m_{TCC} = \sum_{\substack{i=1 \\ i \neq k}}^n c_{i_{TCC}} \cdot V_i + \frac{1}{c_{k_{crea}}} \cdot \left(m_{crea} - \sum_{\substack{i=1 \\ i \neq k}}^n c_{i_{crea}} \cdot V_i \right)$$

After rearrangement eq. 5, ordering with respect to coefficient V_i

$$\text{eq. 6} \quad m_{TCC} = \sum_{\substack{i=1 \\ i \neq k}}^n \left(c_{i_{TCC}} - \frac{c_{k_{TCC}}}{c_{k_{crea}}} \right) \cdot V_i + \frac{c_{k_{TCC}}}{c_{k_{crea}}} \cdot m_{crea}$$

This equation can be extremized in order to give the highest and lowest amount of TCC. Assuming of all sample volumes

$$\text{eq 7} \quad 0.2L \leq V_i \leq 0.7L$$

defining

$$\text{eq 8} \quad D_i = c_{i_{TCC}} - \frac{C_{k_{TCC}}}{C_{k_{crea}}}$$

$m_{TCC \max}$ results by

$$\text{eq 9} \quad m_{TCC \max} = \sum_{\substack{i=1 \\ i \neq k}}^n (c_{i_{TCC}} - D_i) \cdot \bar{V}_i + \frac{C_{k_{TCC}}}{C_{k_{crea}}} \cdot m_{crea} \quad \text{with} \quad \bar{V}_i = \begin{cases} 0.2 & \text{if } D_i \leq 0 \\ 0.7 & \text{if } D_i \geq 0 \end{cases}$$

$m_{TCC \min}$ results by

$$\text{eq 10} \quad m_{TCC \min} = \sum_{\substack{i=1 \\ i \neq k}}^n (c_{i_{TCC}} - D_i) \cdot \bar{V}_i + \frac{C_{TCC}k}{C_{crea}k} \cdot m_{crea} \quad \text{with} \quad \bar{V}_i = \begin{cases} 0.7 & \text{if } D_i \leq 0 \\ 0.2 & \text{if } D_i \geq 0 \end{cases}$$

For a good approximation of the extreme values, k has to be from a sample with a half maximal TCC / creatinine ratio.

Screening of TCC and its metabolites for the potential to inhibit various human enzymes

The influence of TCC and a few of its known metabolites was investigated by incubation of a high concentration) of the compound in a standard battery of *in vitro* assays using preparation of human enzymes (table S6). The effect on the activity of the enzymes was calculated as % inhibition compared to a solvent control. Each assay was performed in triplicate and results were calculated as mean \pm SD. In detail the following enzymes were investigated: Human esterases (hCEs): Baculovirus expressed and purified recombinant human hCE1 and hCE2 were investigated as for inhibition as previously described ⁴. The enzyme hCE3 was used as a cytosolic mixture of proteins obtained from Sf insect cells. Microsomal amidase (FAAH): The inhibition assay performed with baculovirus expressed and purified recombinant human FAAH as described ⁵. Benzil was used as a reference inhibitor for esterase assays (IC_{50} : $0.045 \pm 0.003 \mu\text{M}$ for hCE1; ⁶. Cytochrome P-450 monooxygenases (CYPs): Initial studies for the ability of TCC and its metabolites to inhibit CYPs were performed using human liver microsomes with 7-ethoxyresorufin O-deethylase (EROD) as substrate ⁷. Gluthione-S-transferases (GSTs). The assay was carried out using human liver cytosol as source of GSTs utilizing 1-chloro-2,4-dinitrobenzene (CDNB) as substrate ⁸. Ethacrynic acid was used as a reference inhibitor of GSTs. Mitochondrial epoxide hydrolase (mEH): The mEH enzyme assay was performed as previously described ⁹, using [³H]-*cis*-stilbene oxide as a substrate. Recombinant human mEH was expressed in a baculovirus expression system and prepared as described.¹⁰

Results

Development of an automated analytical method for TCC exposure assessment

Online SPE and LC separation: Crude urine and plasma samples were injected directly into the LC-MS instrument after mixing with I.S. solution and centrifugation (Fig. S2). No breakthrough for the analytes up to an elution volume of more than 6 mL was detected (Fig. S5). Therefore TCC, its metabolites and analogs were fully trapped by the online SPE column. Salts and proteins were directed to waste in an extraction time of only 1.0 min, corresponding to an elution with 30 void volumes of the SPE column. Thereafter, the analytes were eluted in back-flush mode from the SPE-column toward the analytical column. The analytes rapidly eluted from the SPE column in 10-14 sec with a total analysis time of 1.2 min per sample (Fig. S6). While the peak of the most polar 2'SO₃-O-TCC has a very narrow shape, the less polar TCC peak is broader and shows tailing. The transfer step from SPE column to the analytical column is fully completed after 2.8 min total analysis time. At that time, the SPE column is shunt offline the LC-MS/MS to allow its clean-up with 100 % ACN for 2 min and its reconditioning for another 2 min (60 void volumes). During this time, the separation of the analytes proceeded simultaneously on the Acquity RP-18 column. The analytes were baseline separated and eluted at stable retention times (variation \pm 0.03 min) from the column in reverse order of their polarity (Fig. S7 and table 1). The retention time of the 2'OH-TCC peak was surprisingly only slightly shorter than for TCC, although it bears an additional hydroxyl group. This is most likely caused by the formation of an intermolecular hydrogen bond between the hydroxyl group and the urea moiety as reported earlier¹¹. The analytes eluted rapidly (3 minutes; 2-5 min of total analysis time) between the column void volume (120 μ L, first 1.5 min of total analysis time) and the cleaning step at 5-6 min of total analysis time. This optimized online-SPE-LC setup minimized matrix influence on the ESI-MS detection, as demonstrated by the lack of effect of injected plasma and urine in an ion suppression analysis (Fig. S8). TCC perfectly co-eluted with its deuterated I.S. (Fig. S1)

ESI-MS/MS detection: The electrospray ionization of the slightly acidic carbanilides and their phenol and sulfate conjugate derivatives was carried out in negative ion mode detecting the [M-H]⁻ ions of the analytes. TCC and its analogs gave rise to intense fragment ions generated by the fragmentation of both carbon-nitrogen bonds of the urea moiety as described previously (Fig. S9)¹¹⁻¹⁶. The resulting aniline and isocyanate ions are specific and allow deduction of the substitution pattern of both rings of the carbanilides. The abundance of the ions was dependent on the substitution pattern. The [M-H]⁻ of TCC, DCC and 3'Cl-TCC, which are deprotonated in one of the urea nitrogens only lead to the formation of aniline fragment ions (A and B in Fig. S9). Thus, TCC gave rise to strong fragments at *m/z* 160 of the dichloroanilin and *m/z* 126 of the monochloro aniline (Fig. S1 and S9). The I.S. bearing six ¹³C in the monochloro ring consequently formed ions at *m/z* 160 and *m/z* 132. The symmetric DCC and 3'-OH-TCC each gave rise to one highly abundant fragment at *m/z* 126 and *m/z* 160, respectively. In contrast, hydroxylated compounds, presumably deprotonated at either the more acidic phenol or the sulphate group, demonstrate a strong formation of the isocyanate of the substituted

ring at m/z 168 (Fig. S9). The dominating formation of this ion by 2'-OH-TCC and its sulfoconjugate indicates a stabilization of the isocyanate ion by the formation of a five member lactam ring with the neighbouring hydroxyl group at the ring as discussed by Warren et al ¹¹. The 3'-OH-TCC isocyanate can not form such a stabilized ion thus the aniline fragment at m/z 142 of the substituted ring was detected as the most abundant ion. The sites of fragmentation and transitions used for quantification in SRM mode are shown in Fig. S1. The optimized MS parameters are presented in table S1.

Calibration and validation: The method was calibrated using a series of standard solutions, which were treated equally with sample solutions. The limit of detection (LOD, S/N = 3) for TCC and most of the analytes was 0.15 nM (50 pg/mL) equivalent to 6 fmol on the column (Table 1). The detection limit of 3'-Cl-TCC was slightly higher (0.3 nM). The method provided a broad linear range of detection, over 3 orders of magnitude ($r^2 \geq 0.99$). The early eluting metabolites 2'-SO₃-TCC and 3'-OH-TCC showed a slightly more narrow linear range, probably because of a lower extraction efficacy on SPE column for these polar compounds (Table 1). One fundamental drawback inherent to the application of online-SPE is the risk of carry over ¹⁷. In order to investigate carry over, the sample with highest concentration (0.5 μ M) was injected and the TCC in subsequent blank injections was quantified. Because the carry over ($0.12 \pm 0.02\%$, $n = 3$), was in the range of the performance of the auto sampler, interference due to carry over can be ruled out.

In order to validate the method, plasma and urine samples were spiked with 10, 30 and 100 nM of the analytes and processed like the samples. The present method shows a near perfect accuracy for TCC in these crude samples, with a mean recovery rate of $103 \pm 2\%$ for both urine and plasma (table S2). A similar, excellent accuracy was observed for the TCC analogs DCC and 3'-Cl-TCC as well as the metabolites 2'-OH-TCC and 3'-OH-TCC (SI table S2). Dilutions with I.S. solution of 1:1 and 1:4 both yielded good recovery rates indicating the efficiency of the utilized online SPE step for sample preparation. A tendency of overestimation was observed for 2'-SO₃O-TCC which elutes about 2 min before the I.S. An inaccurate accuracy with a mean recovery rate of $134 \pm 6\%$ was found for 1:1 diluted urine samples. In spiked plasma the mean recovery was $115 \pm 7\%$, barely within an acceptable accuracy window of $100 \pm 20\%$. When the 1:4 dilution with I.S. solution was used this matrix effects vanished and the determined recovery rates were with 102 ± 2 and 101 ± 2 for urine and plasma, as accurate as for all other analytes.

In addition to the good accuracy, the method precision was also excellent with an inter sample variation of less than 5% and an intra sample variation of less than 10% for all analytes. Remarkably for TCC, intra- and inter sample variations were $1.1 \pm 0.4\%$ and $2.6 \pm 1.8\%$ respectively (SI table S2). Thus, the direct injection of crude samples after addition of I.S. and centrifugation in the fully automated ultra-fast online-SPE-LC-MS/MS did not compromise the analytical performance and is ideally suited for the exposure measurement of TCC.

Compared to the only other online-SPE-LC-MS/MS method described for the detection of TCC in biological samples, the described approach is not only significantly, but is also significantly more sensitive with an LOD of 0.15 nM compared to 2.9 nM (0.91 ng/mL)

¹². In addition only 50 µl of sample are required for quantification of urine or plasma levels in triplicate. The analysis speed and sensitivity was also comparable to or better than standard LC-MS/MS methods with an analysis time of 10 min and a LOD of 2.9 nM in the sample vial as described by Sapkota et. al. ¹³.

Detection of TCC-N-glucuronides in urine of exposed humans

The LC-ESI(-)-MS scan chromatogram of urine show numerous peaks reflecting the complexity of the matrix (Fig. S10A). The extracted ion chromatogram (XIC) at m/z 489 in unit resolution of the expected $[M-H]^+$ ion of the glucuronides also resulted in several peaks (Fig. S10B). However the peaks of the glucuronides could be identified based on the following assumption: in addition to the $^{35}\text{Cl}_3$ TCC-N-G signal at m/z 489, the glucuronides should form $[M-H]^+$ ions at m/z 491 for the molecule bearing one ^{37}Cl isotope and at m/z 493 for the molecule bearing two ^{37}Cl isotopes. The two peaks eluting around 3.5 min fulfil this criterion and thus can be tentatively identified as TCC-N-G by the combination of this three XIC traces (Fig. S10B). The fragment spectras observed from these peaks are consistent with the suggested structure of the TCC-N-G (Fig. S10D-E). The earlier eluting peak gave rise to intense fragment ions at m/z 336 that would be expected from dichloraniline-glucuronide ion and therefore can be identified as a TCC-N-glucuronide. The second peak showed the same fragment ion of the monochloroaniline side of the molecule at m/z 302 and thus was identified as TCC-N'-glucuronide (Fig. S10). This structure elucidation is verified by the $^{37}\text{Cl}/^{35}\text{Cl}$ ratio of the fragment ions of the $[M-H]^+$ precursor ions of $^{37}\text{Cl}^{35}\text{Cl}_2$ -TCC-N-G at m/z 491. The fragment ions at m/z 304 and m/z 302 of the TCC-N'-glucuronide have a $^{37}\text{Cl}/^{35}\text{Cl}$ ratio of about 0.5 indicating the presence of one chlorine atom in the fragment, whereas the fragment ions of the TCC-N-glucuronide at m/z 338 and m/z 336 show a $^{37}\text{Cl}/^{35}\text{Cl}$ ratio of about 2 and thus demonstrate the presence of two chlorine atoms in that fragment. Based on this fragmentation pattern a LC-ESI-MS method operating in the SRM mode for the selective semi-quantitative detection of the two TCC-N-Gs was developed. This approach provided an excellent selectivity (Supplemental material Fig. S10 C).

References:

1. Gruenke, L. D.; Craig, J. C.; Wester, R. C.; Maibach, H. I.; North-Root, H.; Corbin, N. C., A selected ion monitoring GC/MS assay for 3,4,4'-trichlorocarbanilide and its metabolites in biological fluids. *J Anal Toxicol* **1987**, 11, (2), 75-80.
2. Scharpf, L. G., Jr.; Hill, I. D.; Maibach, H. I., Percutaneous penetration and disposition of triclocarban in man: body showering. *Arch Environ Health* **1975**, 30, (1), 7-14.
3. Mosteller, R. D., Simplified calculation of body-surface area. *N Engl J Med* **1987**, 317, (17), 1098.
4. Shan, G.; Hammock, B. D., Development of sensitive esterase assays based on alpha-cyano-containing esters. *Anal Biochem* **2001**, 299, (1), 54-62.
5. Huang, H.; Nishi, K.; Tsai, H. J.; Hammock, B. D., Development of highly sensitive fluorescent assays for fatty acid amide hydrolase. *Anal Biochem* **2007**, 363, (1), 12-21.
6. Wadkins, R. M.; Hyatt, J. L.; Wei, X.; Yoon, K. J.; Wierdl, M.; Edwards, C. C.; Morton, C. L.; Obenauer, J. C.; Damodaran, K.; Beroza, P.; Danks, M. K.; Potter, P. M., Identification and characterization of novel benzil (diphenylethane-1,2-dione) analogues as inhibitors of mammalian carboxylesterases. *J Med Chem* **2005**, 48, (8), 2906-15.
7. Pohl, R. J.; Fouts, J. R., A rapid method for assaying the metabolism of 7-ethoxyresorufin by microsomal subcellular fractions. *Anal Biochem* **1980**, 107, (1), 150-5.
8. Habig, W. H.; Pabst, M. J.; Jakoby, W. B., Glutathione S-transferases. The first enzymatic step in mercapturic acid formation. *J Biol Chem* **1974**, 249, (22), 7130-9.
9. Gill, S. S.; Ota, K.; Hammock, B. D., Radiometric assays for mammalian epoxide hydrolases and glutathione S-transferase. *Anal Biochem* **1983**, 131, (1), 273-82.
10. Beetham, J. K.; Tian, T.; Hammock, B. D., cDNA cloning and expression of a soluble epoxide hydrolase from human liver. *Arch Biochem Biophys* **1993**, 305, (1), 197-201.
11. Warren, J. T.; Allen, R.; Carter, D. E., Identification of the metabolites of trichlorocarbanilide in the rat. *Drug Metab Dispos* **1978**, 6, (1), 38-44.

12. Ye, X.; Kuklennyik, Z.; Needham, L. L.; Calafat, A. M., Measuring environmental phenols and chlorinated organic chemicals in breast milk using automated on-line column-switching-high performance liquid chromatography-isotope dilution tandem mass spectrometry. *J Chromatogr B* **2006**, 831, (1-2), 110-5.
13. Sapkota, A.; Heidler, J.; Halden, R. U., Detection of triclocarban and two co-contaminating chlorocarbanilides in US aquatic environments using isotope dilution liquid chromatography tandem mass spectrometry. *Environ Res* **2007**, 103, (1), 21-9.
14. Cha, J.; Cupples, A. M., Detection of the antimicrobials triclocarban and triclosan in agricultural soils following land application of municipal biosolids. *Water Res* **2009**, 43, (9), 2522-30.
15. Gonzalez-Marino, I.; Quintana, J. B.; Rodriguez, I.; Cela, R., Simultaneous determination of parabens, triclosan and triclocarban in water by liquid chromatography/electrospray ionisation tandem mass spectrometry. *Rapid Commun Mass Spectrom* **2009**, 23, (12), 1756-66.
16. Garcia-Ac, A.; Segura, P. A.; Viglino, L.; Furtos, A.; Gagnon, C.; Prevost, M.; Sauve, S., On-line solid-phase extraction of large-volume injections coupled to liquid chromatography-tandem mass spectrometry for the quantitation and confirmation of 14 selected trace organic contaminants in drinking and surface water. *J Chromatogr A* **2009**, 1216, (48), 8518-27.
17. Mullett, W. M., Determination of drugs in biological fluids by direct injection of samples for liquid-chromatographic analysis. *J Biochem Biophys Methods* **2007**, 70, (2), 263-73.

Table S1: Mass spectrometric parameters for the ESI(-)-MS/MS detection of the analytes and the I.S. The m/z values of the transitions used for quantification in SRM as well the optimized potentials: Declustering potential (DP), collision energy (CE) and collision cell exit potential (CXP) are shown.

analyte	m/z [M-H] ⁻	m/z product ion	DP (V)	CE (V)	CXP (V)	period
2'SO ₄ -TCC	409	168	-60	-32	-11	1
3'OH-TCC	329	168	-75	-16	-9	1
DCC	279	126	-70	-20	-7	2
2'OH-TCC	329	168	-65	-18	-9	2
TCC	313	160	-75	-20	-9	2
3'Cl-TCC	347	160	-80	-22	-11	2
I.S.	319	160	-70	-20	-7	2

Table S2: Recovery rates determined in spiked and diluted urine and plasma samples (1:1 and 1:4 (v/v) respectively). The mean of the measured concentration, the recovery rate (rec.) and RSD of the analysis of 3 independent samples (intersample variation) are shown. Intrasample variation is presented as the RSD of three non-consecutive injections of the same sample.

Part A

Matrix (spiked content)	dilution	2'SO ₄ -TCC				3'OH-TCC				DCC			
		conc. [nM]	rec. (%)	intra. RSD (%)	inter. RSD (%)	conc. [nM]	rec. (%)	intra. RSD (%)	inter. RSD (%)	conc. [nM]	rec. (%)	intra. RSD (%)	inter. RSD (%)
urine (10 nM)	1:2	13.19	131.9	3.57	1.07	9.97	99.67	2.59	3.07	10.17	101.7	1.97	1.26
	1:5	10.12	101.1	6.14	3.28	9.38	93.77	5.94	2.99	9.74	97.43	3.95	12.85
urine (30 nM)	1:2	42.23	140.8	2.73	2.41	30.64	102.1	1.96	2.33	29.29	97.62	0.72	3.67
	1:5	30.27	100.9	5.95	9.42	30.89	103.0	8.62	5.60	31.22	104.1	1.29	2.95
urine (100 nM)	1:2	129.4	129.4	2.41	1.95	101.1	101.1	3.52	0.39	100.3	100.3	0.56	0.23
	1:5	105.1	105.1	2.57	1.17	99.95	99.95	5.10	7.98	105.2	105.2	1.42	1.92
plasma (10 nM)	1:2	12.31	123.1	2.75	5.37	9.81	98.09	7.71	4.49	10.31	103.1	1.09	1.36
	1:5	10.07	100.7	6.56	5.18	9.55	95.53	6.17	11.80	10.54	105.4	4.74	9.82
plasma (30 nM)	1:2	32.88	109.6	8.99	11.96	30.20	100.7	2.22	6.52	32.40	108.0	1.43	5.49
	1:5	29.93	99.8	2.33	6.97	30.75	102.5	3.09	5.84	33.20	110.7	1.51	1.01
plasma (100 nM)	1:2	114.2	114.2	5.72	6.71	102.2	102.2	1.58	2.81	104.3	104.3	1.94	3.94
	1:5	103.7	103.7	2.27	1.69	96.40	96.40	5.38	5.34	104.2	104.2	1.43	1.94

Part B (Table S2)

Matrix (spiked content)	<i>dilution</i>	2'OH-TCC				TCC				3 Cl-TCC			
		conc. [nM]	rec. (%)	intra. RSD (%)	inter. RSD (%)	conc. [nM]	rec. (%)	intra. RSD (%)	inter. RSD (%)	conc. [nM]	rec. (%)	intra. RSD (%)	inter. RSD (%)
urine (10 nM)	1:2	9.97	99.67	1.19	3.36	10.29	102.9	1.46	1.81	10.53	105.3	3.74	3.42
	1:5	10.96	110.0	2.59	6.03	10.02	100.2	1.69	5.02	11.11	111.1	4.87	15.27
urine (30 nM)	1:2	29.89	99.62	1.42	0.81	31.32	104.4	0.90	0.92	30.96	103.2	2.30	1.94
	1:5	30.22	100.7	5.13	3.08	30.45	101.5	0.54	3.56	31.92	106.4	3.61	6.76
urine (100 nM)	1:2	102.1	102.1	1.90	0.14	105.5	105.5	0.91	1.31	102.1	102.1	1.62	3.38
	1:5	103.5	103.5	1.16	2.80	103.5	103.5	0.94	1.05	104.4	104.4	1.85	1.22
plasma (10 nM)	1:2	9.97	99.73	1.64	4.09	10.37	103.7	1.50	2.52	10.07	100.7	4.55	2.52
	1:5	10.71	107.3	3.72	8.63	10.10	101.0	1.15	6.13	11.30	113.0	9.46	10.69
plasma (30 nM)	1:2	29.80	99.33	1.40	0.67	31.65	105.5	1.63	0.51	30.83	102.8	4.16	5.73
	1:5	29.83	99.44	1.65	4.89	30.17	100.6	0.98	4.42	33.29	111.0	0.85	1.74
plasma (100 nM)	1:2	99.26	99.26	1.08	1.29	105.9	105.9	1.29	2.56	100.0	100.0	7.94	2.84
	1:5	102.5	102.5	0.90	1.95	101.9	101.9	0.57	1.91	104.6	104.6	2.87	0.93

Table S3: Information about the subjects of the human exposure study. The body surface area (BSA) was calculated based on height and weight by the Mosteller formular³.

subject	Sex	Age (years)	Height (cm)	Weight (kg)	BMI (kg/m ²)	BSA (m ²)
A	male	60	182	70	21.1	1.88
B	male	25	173	80	26.7	1.96
C	male	42	170	64	22.1	1.74
D	male	27	170	63	21.8	1.72
E	female	31	172	63	21.3	1.73
F	Male	33	185	77	22.5	1.99
<i>mean±SD</i>		<i>36±13</i>	<i>175±7</i>	<i>70±7</i>	<i>22.6±2.1</i>	<i>1.84±0.12</i>

TableS4: Maximal concentration of TCC in urine after conjugate hydrolysis. The total amount of TCC excreted is estimated based on the assumption that creatinine excretion rate is 1.5 g/24h and a volume of urine excretion of 0.2-0.7 L per urination (formula given in SI material). Taking further in to account that 25% of TCC are renal excreted, the total absorbed TCC was estimated. Based on a soap consumption (11.7 g; 70 µg TCC) this amount is also expressed as % of the total dose applied.

volunteer	C_{\max} TCC		total urinary TCC excretion		absorbed TCC	
	nM	µg/g _{crea}	min-max [µg]	mean [µg]	mg	% of dose
A	751±2.3	200±1.2	95 – 290	192	0.7	1.1
B	1010±14	285±4.5	57 – 331	194	0.8	1.1
C	239±15	42±7.3	15 – 112	63	0.3	0.4
D	116±5.8	77±0.4	21 – 72	47	0.2	0.3
E	167±2.8	88±6.1	86 – 190	138	0.6	0.8
F	119±7.2	47±2.3	14 – 42	28	0.1	0.2
<i>mean±SE</i>	<i>400±160</i>	<i>122±40</i>	<i>14 – 331</i>	<i>110±30</i>	<i>0.5±0.1</i>	<i>0.6±0.2</i>

Table S5: The ratio of epoxy to dihydroxy fatty acids of arachidonate (C20:4, A) and docosahexanoate (C22:6, B) oxylipins in rat plasma following topical treatment of a dose of 1.5 mg/kg BW and 4 mg/kg BW compared with a group treated with vehicle. Two hours following treatment with 1 % TCC containing cream, the plasma concentration of epoxides and dihydroxy fatty acids were monitored as a measure of sEH activity. Neither the group receiving 1.5 mg/kg BW, a comparable dose to exposure by soap nor the high dose group at 4 mg/KG BW showed a significant increase in the ratio of epoxy to dihydroxy fatty acids, indicating that these treatments did not alter sEH activity.

Precursor fatty acid	Epoxid/Diol ratio	Control		TCC 1.5 mg/kg BW		TCC 4 mg/kg BW	
		nM	SE	nM	SE	nM	SE
Linoleate (18:2)	9(10)-EpOME/9,10-DiHOME	0.68	0.12	0.69	0.18	0.67	0.05
	12(13)-EpOME/12,13-DiHOME	0.83	0.20	0.85	0.28	1.00	0.19
alpha-Linolenate (18:3)	9(10)-EpODE/9,10-DiHODE	0.41	0.11	0.55	0.12	0.52	0.05
	12(13)-EpODE/12,13-DiHODE	0.76	0.31	0.99	0.13	0.78	0.15
Arachidonate (20:4)	8(9)-EpETrE/8,9-DiHETrE	2.99	0.42	2.98	0.83	3.21	0.25
	11(12)-EpETrE/11,12-DiHETrE	2.15	0.27	2.16	0.72	2.52	0.23
	14(15)-EpETrE/14,15-DiHETrE	2.11	0.49	2.17	0.80	2.16	0.55
Eicosapentanoate (20:5)	11(12)-EpETE/11,12-DiHETE	1.37	0.31	1.52	0.37	1.69	0.13
	14(15)-EpETE/14,15-DiHETE	0.94	0.48	1.07	0.27	1.29	0.50
	17(18)-EpETE/17,18-DiHETE	1.17	0.27	1.67	0.25	1.63	0.19
Docosahexanoate (22:6)	10(11)-EpDPE/10,11-DiHDPE	5.13	1.79	4.70	1.69	5.10	0.71
	13(14)-EpDPE/13,14-DiHDPE	2.81	0.43	3.34	3.27	3.23	0.15
	16(17)-EpDPE/16,17-DiHDPE	1.12	0.71	0.94	0.33	1.16	0.22
	19(20)-EpDPE/19,20-DiHDPE	0.47	0.18	0.49	0.11	0.58	0.30

Table S6: Screening of TCC and its metabolites for non-intended effects on the activity of human enzymes. Shown is the (%) of inhibition of human carboxylesterases (hCEs), microsomal amidase (FAAH), Cytochrome P-450 monooxygenases (CYP) in EROD assay, glutathione-S-transferases (GSTs) and mitochondrial epoxyde hydrolase (mEH) at compound concentrations from 1-100 μ M. Values represent mean \pm SD of threefold determinations. Neither TCC nor its metabolites 2'OH-TCC and 2'-SO₃O-TCC exhibited a relevant inhibition of any of these enzymes. The results do not indicate that the activity of these enzymes may be influenced by human exposure to TCC. However, since standard colorimetric assays with human cell fractions as enzyme source were utilized for the investigation of CYP and GST activity an effect on specific isoforms of these enzymes can not be excluded.

	hCE1	hCE2	hCE3	FAAH	EROD	GSTs	mEH
test conc.(μ M)	1	1	1	10	100	10	100
	(% inhibition)						
TCC	13 \pm 6	12 \pm 4	<1	<1	13 \pm 4	<1	< 5
2'OH-TCC	22 \pm 6	11 \pm 5	<1	3.5 \pm 0.4	3 \pm 3	3.5 \pm 0.4	< 5
2'SO ₃ -O-TCC	13 \pm 4	8 \pm 1	<1	<1	32 \pm 2	<1	< 5
Benzil ^a	95 \pm 3	78 \pm 1	45 \pm 2	- ^b	- ^b	- ^b	- ^b
Ethacrynic acid ^a	- ^b	- ^b	- ^b	53 \pm 13	- ^b	53 \pm 13	- ^b

^aBenzil and ethacrynic acid are the reference inhibitors of hCE1 and GSTs, respectively. ^bNot tested.

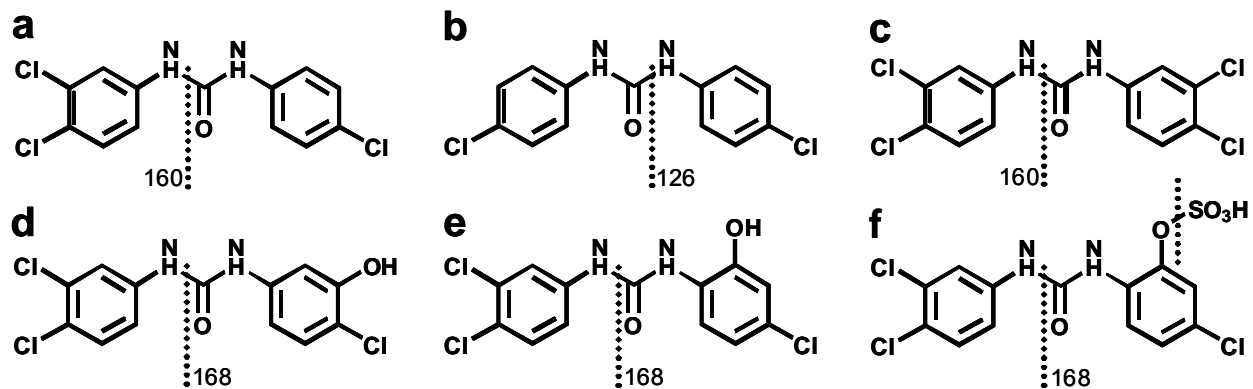


Fig. S1: Chemical structures of the investigated analytes: **a** TCC, **b** DCC, **c** 3'-Cl-TCC, **d** 3'-OH-TCC, **e** 2'-OH-TCC and **f** 2'-SO₄-TCC. The dashed lines illustrate the suggested fragmentation sites while the adjacent numbers represent the m/z values of the fragments used for quantification in SRM.

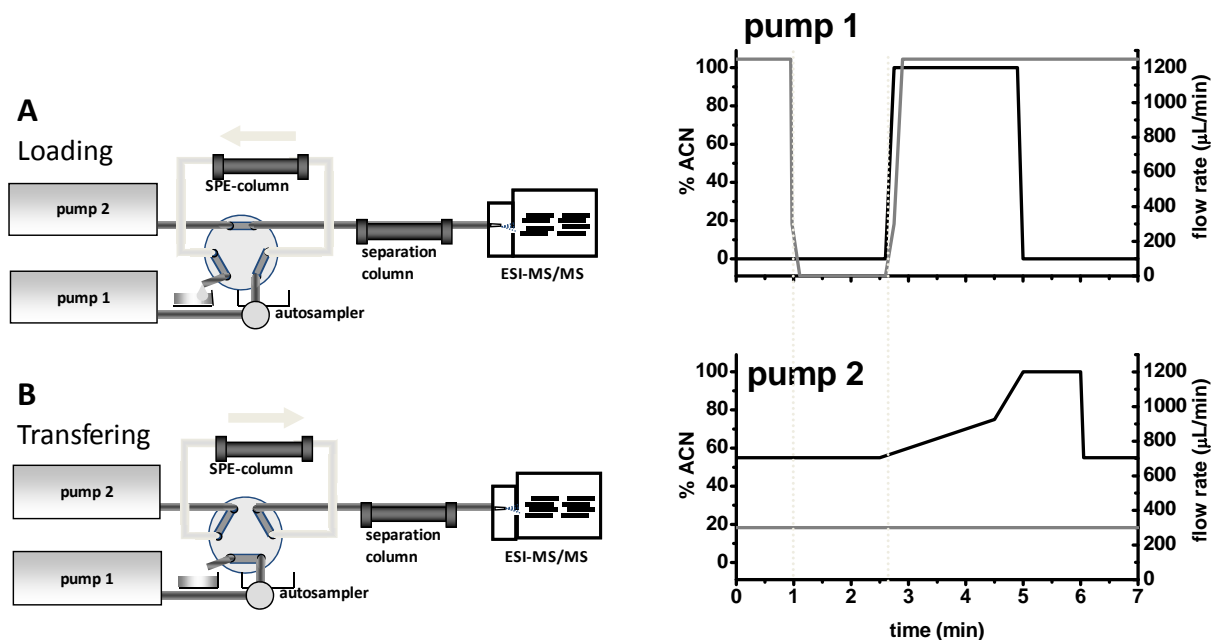


Fig. S2: Scheme of the online-SPE-LC-MS/MS set up. The sample is transferred onto the SPE column by pump 1 (**A**). After this loading step, the six port valve is switched (1.0 min) so that the analytes are eluted from the SPE column towards the separation column by pump 2 (**B**). The valve is switched back immediately after (2.8 min). The analytes elute, while the SPE column is cleaned and regenerated. In the diagrams the applied gradients (black line) and flow rates (gray line) of the LC-pumps are shown. The switching points of the six port valve are indicated by the dashed lines.

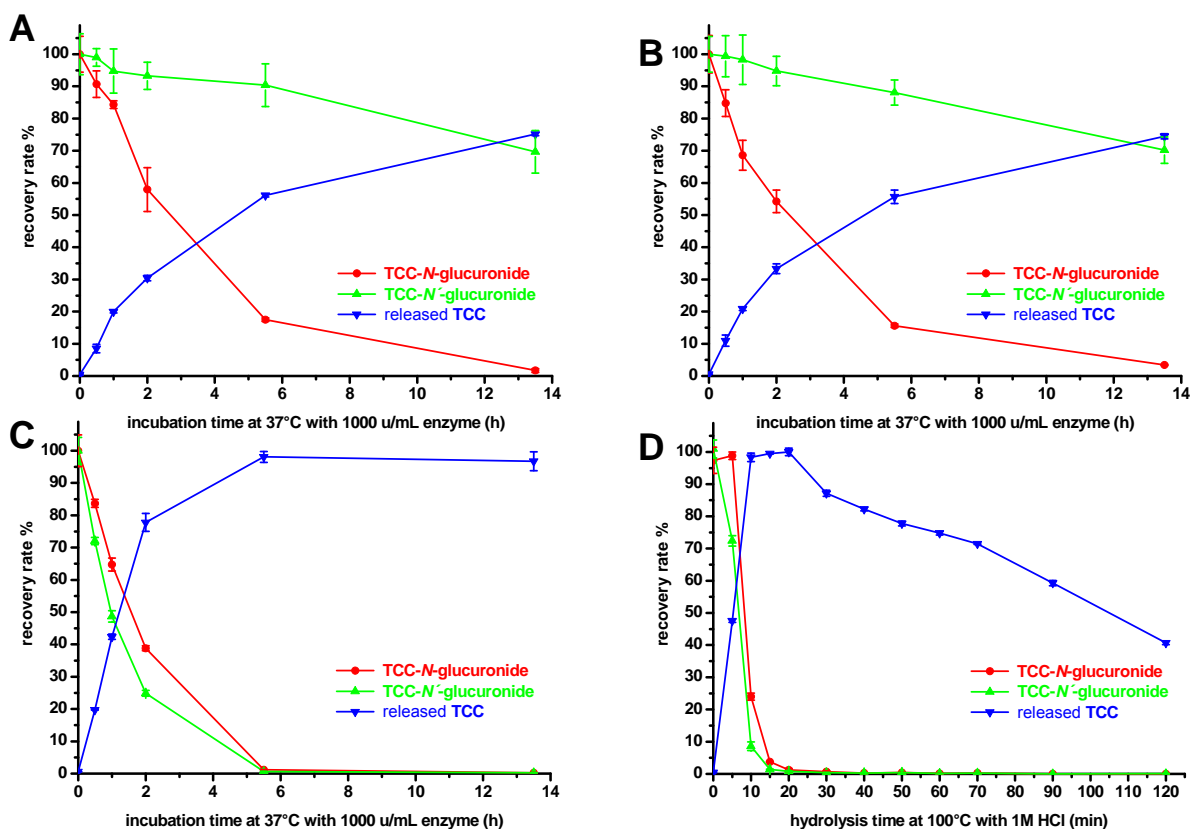


Fig. S3: Hydrolysis of *N*-glucuronides by enzyme and acid treatment. The progression of the hydrolysis was followed over the incubation period by the peak areas of the two *N*-Glucuronides and the released TCC concentration in the urine of an exposed human subject (volunteer A, sampled 5.3 h post exposure). The values for the *N*-glucuronides were normalized as the percent of control sample at 0 min incubation and set to 100%. The TCC concentration in all diagrams is given as % of the highest measured release of TCC (20 min, acid hydrolysis). The mean and the standard deviation of three injections are presented **A**. Incubation with β -glucuronidase from *Helix pomatia* type HP-1. **B**. Incubation with β -glucuronidase from *Helix pomatia* type HP-2. **C**. Incubation with with β -glucuronidase from *Escherichia coli* type V-A. **D**. Acid conjugate hydrolysis at 100 °C with 1 M HCl.

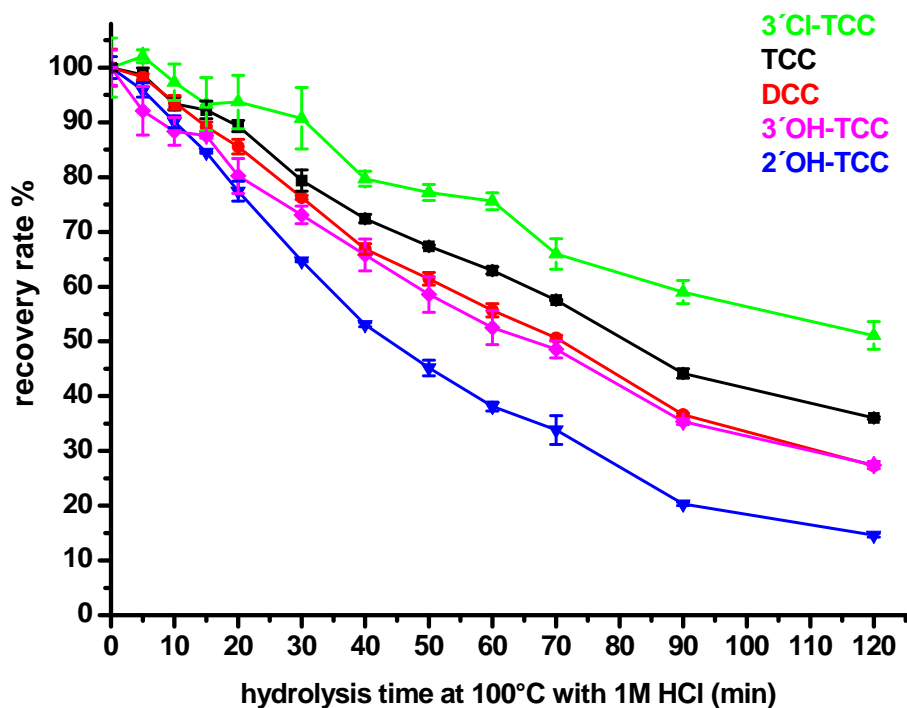


Fig. S4: Degradation of TCC and its analogs by acid hydrolysis. A spiked blank urine sample containing 300 nM of each analyte was incubated with 1 M HCl at 100 °C. The concentration normalized as % of the untreated sample for 3'Cl-TCC, TCC, DCC, 3'OH-TCC and 2'-OH DCC are demonstrated. Data are expressed as the mean \pm standard deviation from three injections.

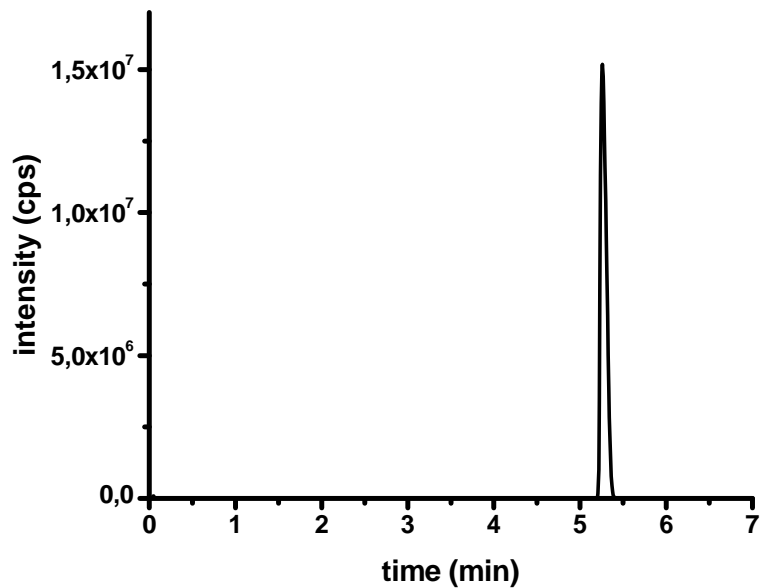


Fig. S5: Break through test of the SPE column. A multi-standard solution (20 μ l of 500 nM in 50 % ACN 1 % HAC) was injected into the loading flow of 1250 μ l/min containing 99.9 % water and 0.1 % HAC. The eluent of the SPE was monitored by ESI(-)-MS/MS. After 5 minutes the solvent was changed to 100 % ACN within 0.2 min in order to elute the trapped analytes. The sum of the SRM signals of the analytes is presented.

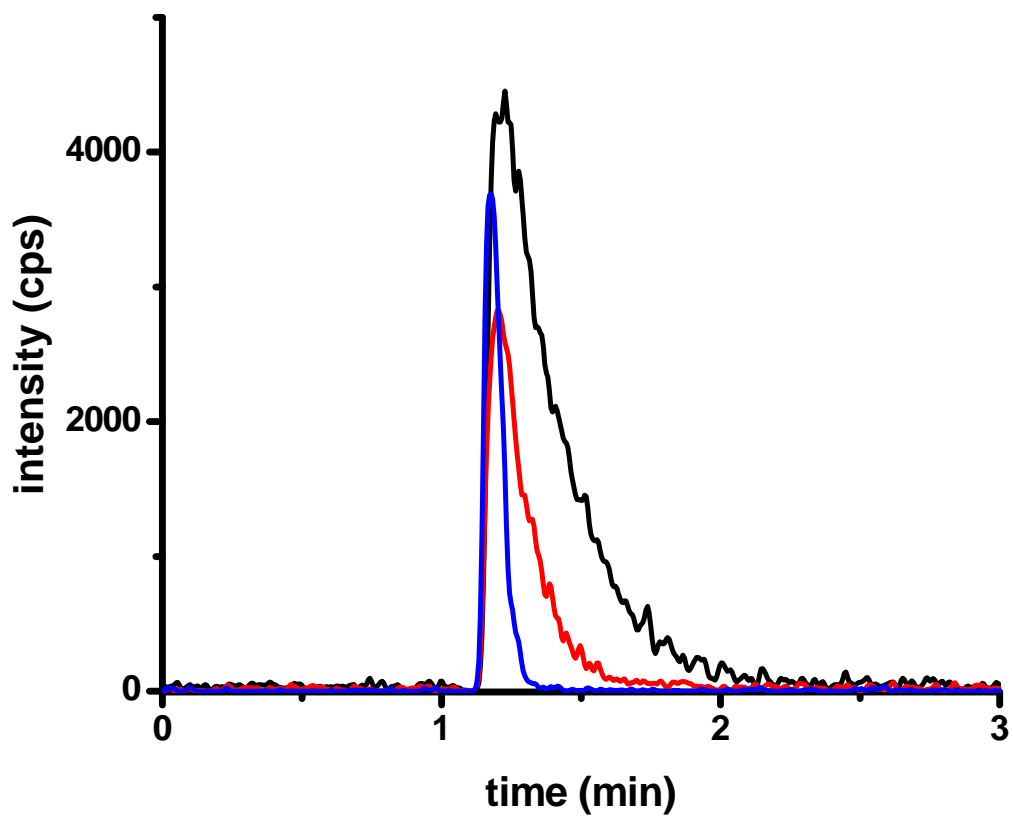


Fig. S6: Elution profile of analytes from the SPE column. The separation column (Fig. S2) was removed from the setup and the eluent of the SPE was directly monitored by ESI(-)-MS/MS. The SRM traces for 2-SO₄-TCC (blue), DCC (red) and TCC (black) of an injection (20 μ l) of a 5 nM standard solution are presented.

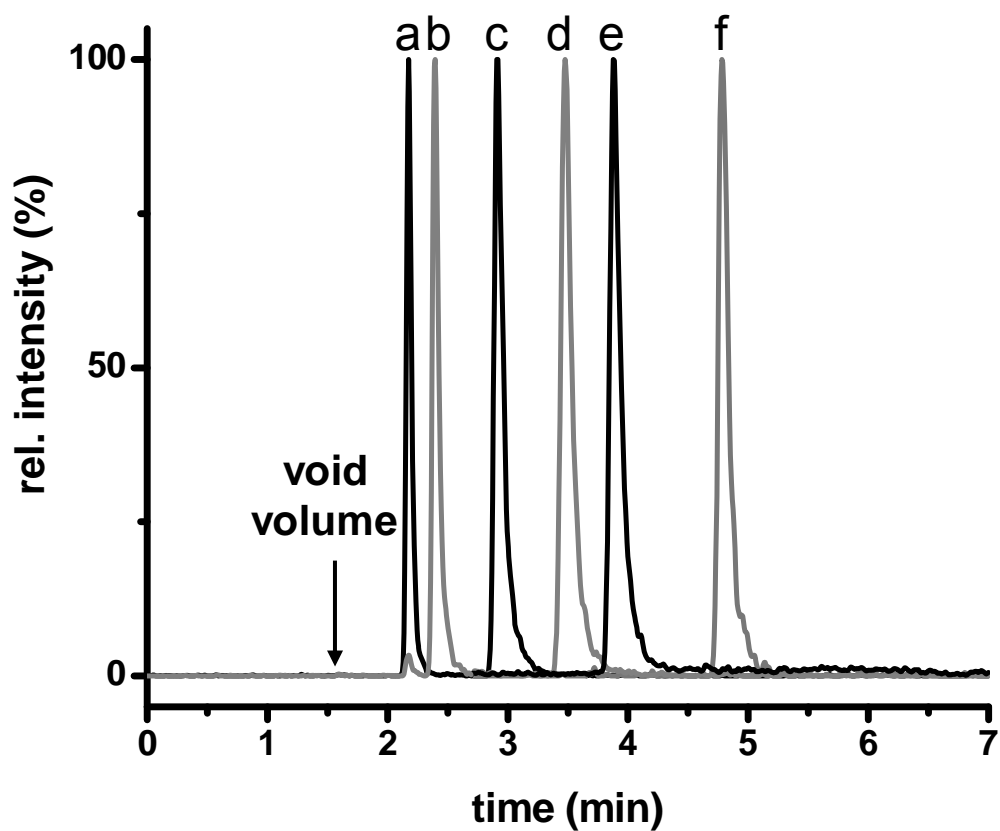


Fig. S7: Separation efficiency of the online-SPE-LC-MS/MS system. The normalized SRM chromatograms of an injection of 20 μ l of a 5 nM standard solution (0.1 pmol on column) are presented. **a** 2'SO₄-TCC, **b** 3'OH-TCC, **c** DCC, **d** 2'OH-TCC, **e** TCC and **f** 3 Cl-TCC.

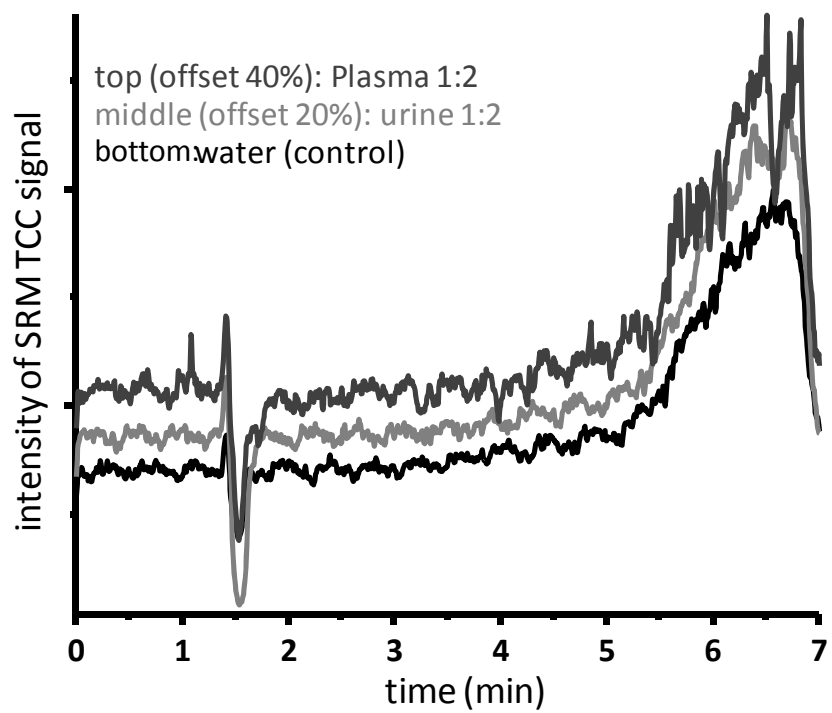
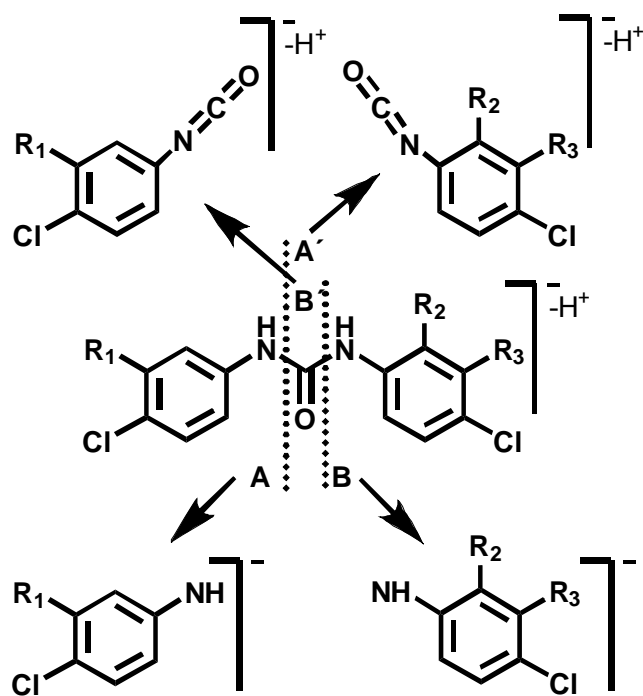


Fig. S8: Ion suppression analysis. The separation column eluent was mixed with a flow of TCC solution (1 pmol/min). The SRM signal of injections (20 μ l) of water and 1:2 diluted blank plasma and urine samples are presented.



compound	R ₁	R ₂	R ₃	fragment <i>m/z</i> (rel. intensity %)			
				A	A'	B	B'
TCC	Cl	H	H	160 (100)	n.d.	126 (15)	n.d.
DCC	H	H	H	126 (100)	n.d.	126 (100)	n.d.
3'-Cl-TCC	Cl	H	Cl	160 (100)	n.d.	160 (100)	n.d.
2'-OH-TCC	Cl	OH	H	160 (1)	168 (100)	142 (48)	n.d.
3'-OH-TCC	Cl	H	OH	160 (40)	168 (68)	142 (100)	n.d.
2-SO ₃ -TCC	Cl	O-SO ₃	H	160 (2)	n.d. 168 (100) *	222 (21) 142 (79) *	n.d.

* additional loss of SO₃

Fig. S9: Fragmentation behavior of TCC and its analogues. Fragmentation occurs at both carbon-nitrogen bonds of the urea leading to four possible fragments. The *m/z* and the relative intensities of the fragments are also presented.

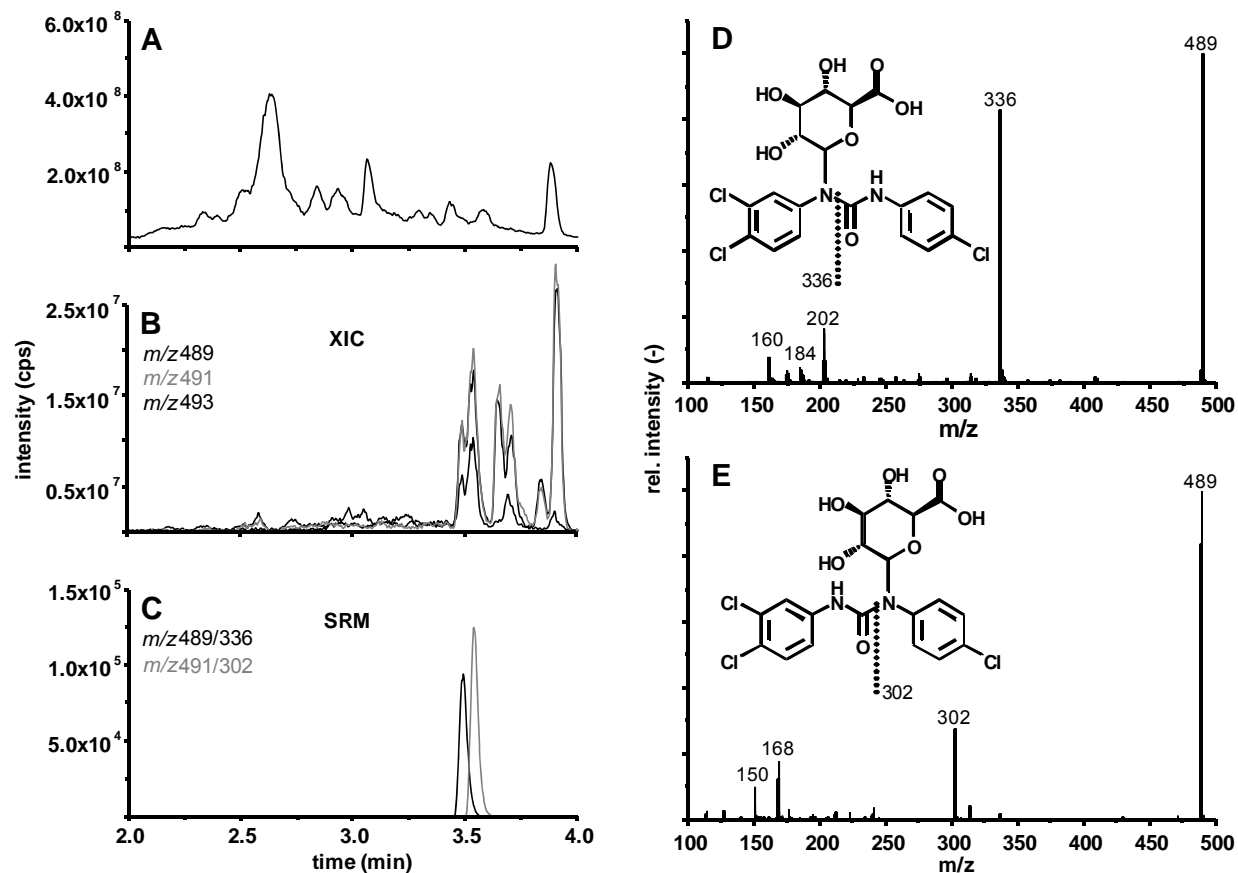


Fig. S10: Detection of TCC *N*-glucuronides in urine. Representative examples of an LC-ESI(-)-MS fullscan (A), XIC at the *m/z* of the different chlorine isotopes of the molecule (B) and SRM chromatogram (C). The fragment spectra of the glucuronides (on the right) are shown together with the corresponding structure. The dashed lines represent sites of fragmentation leading to the most intense fragment ions.

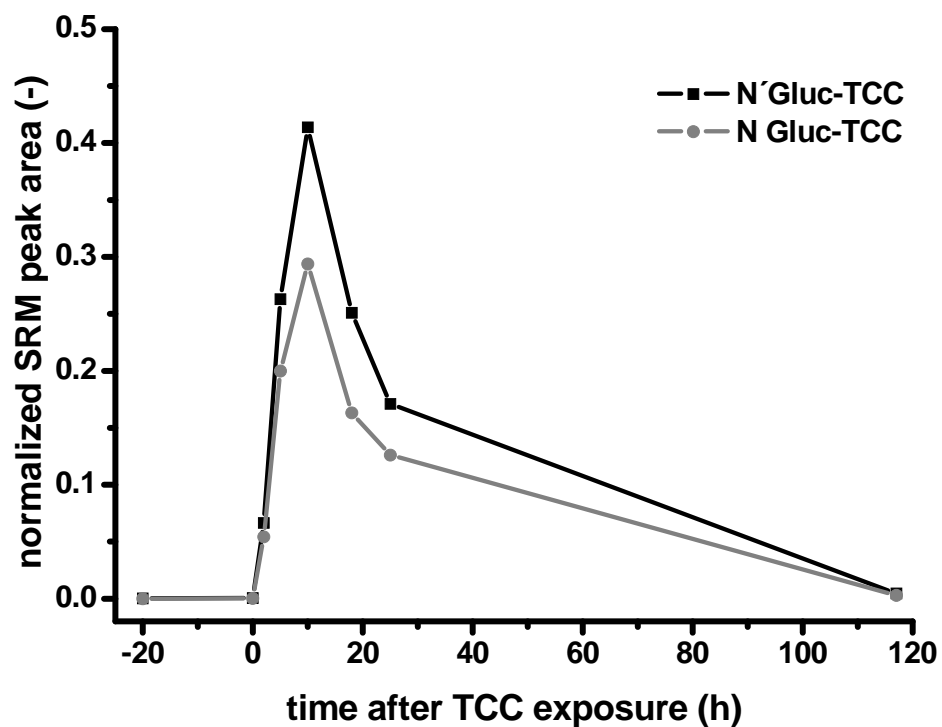


Fig. S11: Qualitative profile of *N*-glucuronides of TCC in urine. The observed area for the glucuronides in SRM mode was normalized by dividing by the area of the I.S. and creatinine content. A representative exemplar profile for volunteer B is presented.

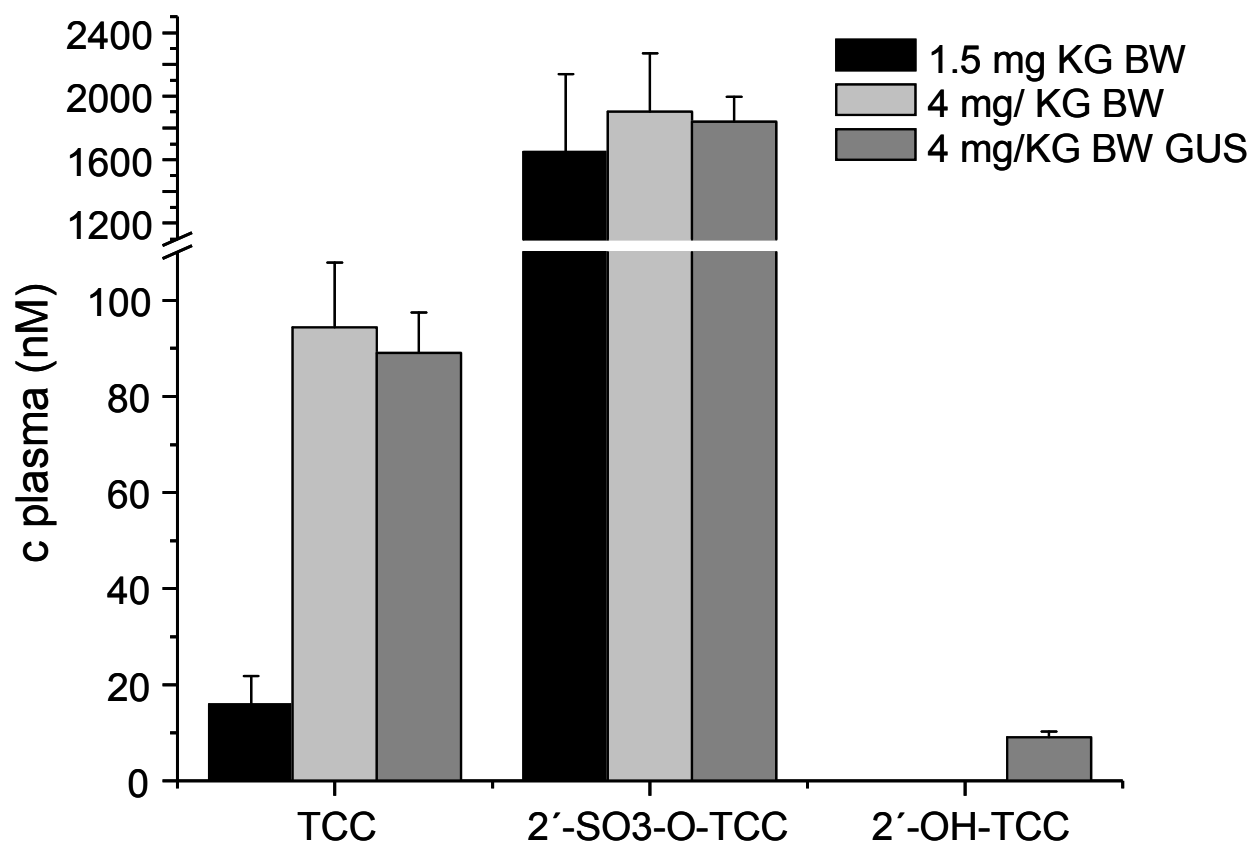


Fig. S12 Plasma concentration of TCC and its metabolites 2'-SO₃-O-TCC and 2'-OH-TCC, 2 h following topical dosing in rats (1.5 mg/kg BW and 4 mg/kg BW). The samples from the high dose group were additionally treated with glucuronidase (GUS) from *E. coli*. The resulting data indicate that the rat produce little or any of the TCC-N-Gs. Mean and standard error from 4 animals per group is presented.

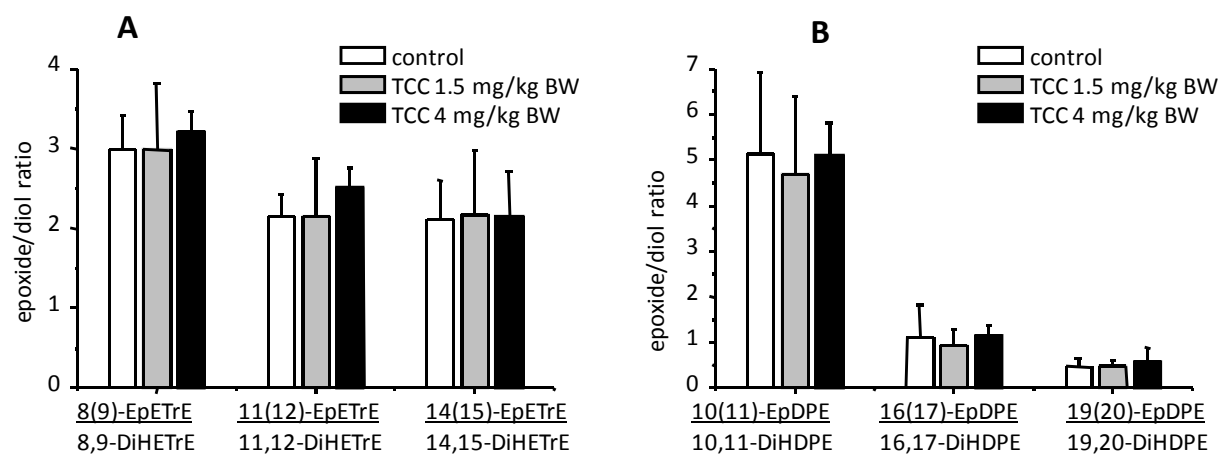


Fig. S13: The ratio of epoxy to dihydroxy epoxy fatty acids of arachidonate (C20:4, **A**) and docosahexanoate (C22:6, **B**) oxylipins in rat plasma following topical treatment of a dose of 1.5 mg/kg BW and 4 mg/kg BW compared with a group treated with vehicle. Ratios are displayed as mean and SE from 4 animals per group.